Acta Crystallographica Section B
**Structural Science**
ISSN 0108-7681

# *Trans*-cinnamic acid and coumarin-3-carboxylic acid: experimental charge-density studies to shed light on [2 + 2] cycloaddition reactions

**Judith A. K. Howard,[a] Mary F. Mahon,[b]* Paul R. Raithby[b] and Hazel A. Sparkes[a]***

[a]Department of Chemistry, University Science Laboratories, Durham University, South Road, Durham DH1 3LE, England, and [b]Department of Chemistry, University of Bath, Claverton Down, Bath BA2 7AY, England

Correspondence e-mail: m.f.mahon@bath.ac.uk, h.a.sparkes@durham.ac.uk

Received 27 October 2008
Accepted 13 January 2009

As part of an ongoing series of experimental charge-density investigations into the intra- and intermolecular interactions present in compounds which undergo solid-state [2 + 2] cycloaddition reactions, the charge-density analyses of *trans*-cinnamic acid and coumarin-3-carboxylic acid are reported. Thus, high-resolution single-crystal X-ray diffraction data were recorded at 100 K for *trans*-cinnamic acid ($\sin\theta/\lambda_{max}$ = 1.03 Å$^{-1}$) and coumarin-3-carboxylic acid ($\sin\theta/\lambda_{max}$ = 1.19 Å$^{-1}$). In addition to the anticipated O—H···O hydrogen bonds weak C—H···O interactions were identified in both structures along with very weak intermolecular interactions between pairs of molecules that undergo solid-state [2 + 2] cycloaddition reactions upon irradiation.

## 1. Introduction

Accurate, high-resolution X-ray charge-density experiments provide information on the electron distribution within the system under study, allowing both the nature of the bonding and the atomic interactions to be determined (Scheins *et al.*, 2005). To this end, Bader's quantum theory of atoms in molecules (AIM; Bader, 1990) is a powerful tool, which characterizes the chemical interactions between atoms on the basis of the topological properties of the electron density and the associated Laplacian at bond-critical points (b.c.p.s). In organic molecules, covalent bonds are classified as shared-shell, while van der Waals and hydrogen-bonding interactions are classified as closed-shell.

In the 1960s, Schmidt and co-workers (Schmidt & Cohen, 1964) carried out a pioneering study into the solid-state reactivity of *trans*-cinnamic acid and its derivatives working on the postulate that '*a reaction in the solid state occurs with a minimum amount of atomic or molecular movement*'. They concluded that for a solid state [2 + 2] cycloaddition reaction to occur the potentially reactive double bonds should be parallel and separated by a maximum of 4.2 Å. Subsequently, a significant number of exceptions to the rule have been identified with molecules that do not fulfill these criteria dimerizing (Ramamurthy & Venkatesan, 1987), while others with short C═C separations remain inert even under prolonged irradiation. Although further studies have been conducted on solid-state [2 + 2] cycloaddition reactions, the reasons why some molecules react while others do not are still not fully understood.

It is postulated that the presence of strong intra- or intermolecular interactions in the reactant may affect the ability of a compound to undergo a [2 + 2] cycloaddition reaction, particularly if these crucial interactions cannot be maintained in the irradiation product (Mahon *et al.*, 2008). The current study forms part of a series of charge-density experiments that

aim to examine the intra- and intermolecular interactions present in compounds which undergo solid-state [2 + 2] cycloaddition reactions. In this context, both *trans*-cinnamic acid and coumarin-3-carboxylic acid are known to undergo photochemically induced solid-state [2 + 2] cycloaddition reactions (Enkelmann *et al.*, 1993; Mahon *et al.*, 2008), see Fig. 1. Herein, the experimental low-temperature single-crystal X-ray diffraction charge-density analyses of both *trans*-cinnamic acid and coumarin-3-carboxylic acid are reported.

## 2. Experimental

### 2.1. Recrystallization

Single crystals suitable for charge-density analysis were obtained by recrystallization of the samples of *trans*-cinnamic acid (1*a*) and coumarin-3-carboxylic acid (2*a*) obtained from Sigma Aldrich. Crystals of (1*a*) were obtained by evaporation from methanol, while (2*a*) crystals were obtained by evaporation from acetonitrile.

### 2.2. Data collection and spherical atom refinement

Single-crystal X-ray diffraction data were collected on an Oxford Diffraction Gemini A Ultra diffractometer using graphite-monochromated Mo $K\alpha$ radiation ($\lambda$ = 0.71073 Å) at 100 (2) K. The data were collected and integrated using Oxford Diffraction *CrysAlis* software. Data were subsequently merged using *SORTAV* (Blessing, 1997) within the *WinGX* suite (Farrugia, 1999). For (1*a*) data were 99% complete to sin $\theta/\lambda$ = 1.02 Å$^{-1}$, with all of the missing data above sin $\theta/\lambda$ = 0.90 Å$^{-1}$. Data for (2*a*) were 99.8% complete up to sin $\theta/\lambda$ = 1.19 Å$^{-1}$. The structures were solved using direct methods (*SHELXS*97; Sheldrick, 2008) and refined by full-matrix least-squares on $F^2$ (*SHELXL*97; Sheldrick, 2008). H atoms were located in the difference-Fourier map and allowed to refine freely. The structures for (1*a*) (Ladell *et al.*, 1956) and (2*a*) (Dobson & Gerkin, 1996) were consistent with those previously reported, see Figs. 2 and 3.

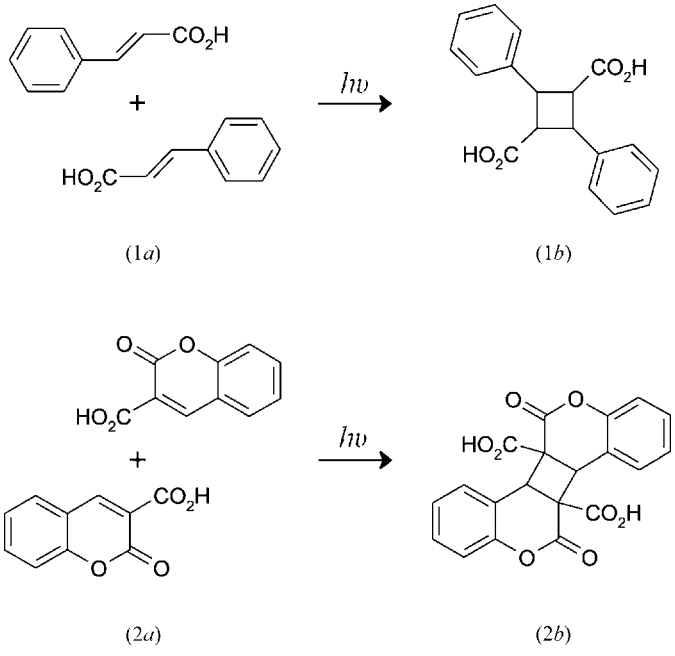


**Figure 1**
Illustration of the photochemical [2 + 2] cycloaddition reactions of *trans*-cinnamic acid (1*a*) and coumarin-3-carboxylic acid (2*a*).

### 2.3. Multipole refinement

The *XD*2006 program suite (Volkov *et al.*, 2006), which implements the multipole formalism of Hansen & Coppens (1978), was used for an aspherical atom refinement, based on the spherical-atom model already obtained. The anisotropic displacement parameters for the H atoms were estimated using the *SHADE*2 web server (Madsen, 2006) and fixed throughout the refinement. Initially the scale factor was refined, followed by the atomic positions and displacement parameters. Subsequently, a high-order refinement (sin $\theta/\lambda$ > 0.7 Å$^{-1}$) was carried out to determine the best atomic positions and displacement parameters for the C and O atoms. This was followed by a low-order refinement (sin $\theta/\lambda$ < 0.7 Å$^{-1}$) of the positional parameters for the H atoms. In all subsequent refinement cycles, the C—H and O—H bond

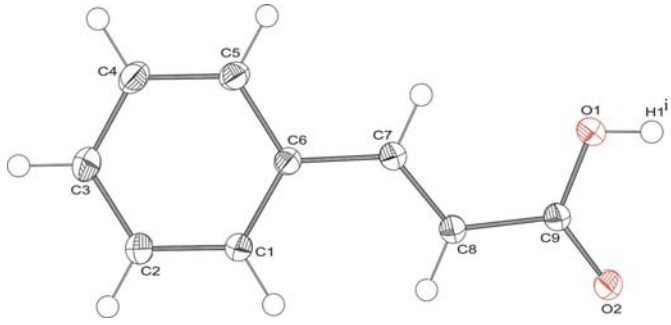


**Figure 2**
*ORTEP* plot of *trans*-cinnamic acid (1*a*) with ellipsoids depicted at the 50% probability level. H atoms are shown as spheres of arbitrary radius.

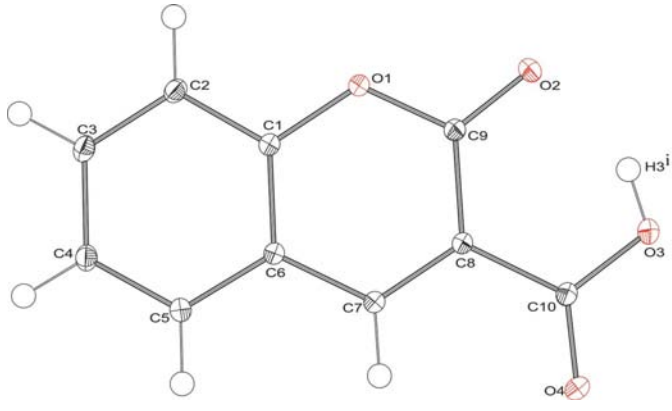


**Figure 3**
*ORTEP* plot of coumarin-3-carboxylic acid (2*a*) with ellipsoids depicted at the 50% probability level. H atoms are shown as spheres of arbitrary radius.

**Table 1**
Crystal data and structural refinement details for *trans*-cinnamic acid (1*a*) and coumarin-3-carboxylic acid (2*a*).

| | (1*a*) | (2*a*) |
|---|---|---|
| Crystal data | | |
| Chemical formula | $C_9H_8O_2$ | $C_{10}H_6O_4$ |
| $M_r$ | 148.15 | 190.15 |
| Cell setting, space group | Monoclinic, $P2_1/n$ | Monoclinic, $P2_1/n$ |
| Temperature (K) | 100 | 100 |
| $a, b, c$ (Å) | 5.5504 (1), 17.5427 (1), 7.7161 (1) | 11.1992 (1), 5.4662 (1), 13.7267 (2) |
| $\beta$ (°) | 96.296 (1) | 107.256 (1) |
| $V$ (Å$^3$) | 746.78 (2) | 802.49 (1) |
| $Z$ | 4 | 4 |
| $D_c$ (Mg m$^{-3}$) | 1.318 | 1.574 |
| $\mu$ (mm$^{-1}$) | 0.093 | 0.124 |
| $F(000)$ | 312 | 392 |
| Crystal size (mm$^3$) | 0.57 × 0.36 × 0.10 | 0.29 × 0.52 × 0.67 |
| Reflections collected | 70 528 | 147 662 |
| Independent reflections | 6591 | 11 309 |
| $R_{int}$ | 0.023 | 0.023 |
| Completeness to $\theta_{max}$ (%) | 99 | 99.8 |
| Spherical-atom refinement | | |
| No. of data in refinement | 6591 | 11 309 |
| No. of refined parameters | 132 | 151 |
| GOF ($F^2$) | 1.022 | 1.036 |
| Final $R_1$ [$F^2 > 2\sigma(F)$] | 0.0376 | 0.0304 |
| $wR_2$† [$F^2 > 2\sigma(F)$] | 0.1223 | 0.1032 |
| Largest difference peak/hole (e Å$^{-3}$) | 0.615/−0.205 | 0.649/−0.248 |
| Multipole refinement | | |
| No. of data in refinement ($N_{ref}$) | 4859 | 8933 |
| No. of refined parameters ($N_v$) | 295 | 367 |
| $N_{ref}/N_v$ | 16.4712 | 24.3406 |
| GOF ($F$) | 1.7414 | 1.6688 |
| Final $R_1$ [$I > 3\sigma(I)$] | 0.0180 | 0.0164 |
| $wR_2$‡ [$I > 3\sigma(I)$] | 0.0143 | 0.0139 |
| Largest difference peak/hole (e Å$^{-3}$) | 0.128/−0.126 | 0.151/−0.138 |

† $w = 1/[\sigma^2(F_o^2) + (aP)^2 + bP$, where $P = [2F_c + \max(F_o^2, 0]/3$. ‡ $w_1 = [F \times (w_2)^{1/2} + \alpha]^2$, where $\alpha = 0$ if $\beta < 0$, $\alpha = \beta^{1/2}$ if $\beta > 0$ with $\beta = (F^2 \times w_2) + (w_2)^{1/2}$.

**Table 2**
Topological properties at the b.c.p.s and r.c.p.s in (1*a*).

| Bond | $d$ (Å) | $R_{ij}$ (Å)† | $\rho(r)$ (e Å$^{-3}$) | $\nabla^2\rho(r)$ (e Å$^{-5}$) | $\epsilon$ |
|---|---|---|---|---|---|
| C1—C2 | 1.3911 (3) | 1.3911 | 2.20 (1) | −20.58 (2) | 0.20 |
| C1—C6 | 1.4038 (3) | 1.4038 | 2.14 (1) | −18.66 (2) | 0.21 |
| C2—C3 | 1.3943 (4) | 1.3943 | 2.12 (1) | −19.13 (3) | 0.22 |
| C3—C4 | 1.3946 (4) | 1.3947 | 2.15 (1) | −18.92 (3) | 0.23 |
| C4—C5 | 1.3926 (4) | 1.3926 | 2.19 (1) | −19.99 (3) | 0.20 |
| C5—C6 | 1.4024 (3) | 1.4025 | 2.13 (1) | −18.73 (2) | 0.19 |
| C6—C7 | 1.4630 (3) | 1.4632 | 1.88 (1) | −14.73 (2) | 0.13 |
| C7—C8 | 1.3446 (3) | 1.3446 | 2.35 (1) | −23.96 (3) | 0.30 |
| C8—C9 | 1.4690 (3) | 1.4692 | 1.91 (1) | −16.04 (2) | 0.17 |
| C9—O1 | 1.3087 (4) | 1.3087 | 2.45 (2) | −29.9 (1) | 0.10 |
| C9—O2 | 1.2447 (4) | 1.2448 | 2.76 (2) | −30.5 (1) | 0.11 |
| C1—H1 | 1.08 | 1.08 | 1.82 (1) | −16.38 (4) | 0.07 |
| C2—H2 | 1.08 | 1.08 | 1.84 (1) | −16.82 (4) | 0.10 |
| C3—H3 | 1.08 | 1.08 | 1.83 (1) | −17.43 (5) | 0.06 |
| C4—H4 | 1.08 | 1.08 | 1.84 (1) | −16.51 (4) | 0.07 |
| C5—H5 | 1.08 | 1.08 | 1.83 (1) | −16.66 (5) | 0.05 |
| C7—H7 | 1.08 | 1.08 | 1.79 (1) | −16.55 (5) | 0.06 |
| C8—H8 | 1.08 | 1.08 | 1.83 (1) | −17.42 (5) | 0.10 |
| O1—H1*A* | 1.01 | 1.01 | 1.84 (2) | −22.7 (1) | 0.00 |
| Ring | | | | | |
| 1(1*a*)‡ | | | 0.18 | 3.3 | |

† $R_{ij}$ is the length of the bond path between atoms. ‡ Ring 1(1*a*) = C1—C2—C3—C4—C5—C6.

lengths were reset to their average neutron diffraction distances of 1.08 and 1.01 Å, respectively. The multipole expansion was truncated at the octupole level for the C and O atoms, while a monopole and a bond-directed dipole were employed for the H atoms. In the case of *trans*-cinnamic acid, five $\kappa$ parameters were refined with five $\kappa'$ parameters for the non-H atoms, while for coumarin-3-carboxylic acid, seven $\kappa$ (including one for the H atoms) and six $\kappa'$ parameters were refined for the non-H atoms. The residual electron-density maps showed no significant features and are presented in the supplementary information (Figs. S2*a* and S2*b*).[1] The Hirshfeld rigid-bond test (Hirshfeld, 1976) carried out after the multipole refinement was satisfactory, with maximum mean-square atomic displacements along the bond directions converging to less than 0.001 Å$^2$ in both cases. Further details of the experimental data collection and refinement are provided in Table 1.

## 3. Results

### 3.1. *Trans*-cinnamic acid (1*a*)

All anticipated intramolecular b.c.p.s were identified, along with a ring-critical point (r.c.p.) for the aromatic ring (C1–C6); their associated charge densities and Laplacians are listed in Table 2. It is possible to obtain a quantitative comparison of the covalent bond strengths by examining the values of the topological properties at their respective b.c.p.s (Bader *et al.*, 1982). As would be expected, the six C—C bonds around the aromatic ring are of a similar strength, on the basis of their topological properties, with a small range of values observed for $\rho(r)$ at the b.c.p.s (2.12–2.20 e Å$^{-3}$). In addition, their $\nabla^2\rho(r)$ and $\epsilon$ values are very similar to each other and consistent with those seen previously for delocalized aromatic C—C bonds (Hibbs *et al.*, 2003). The C7═C8 double bond at 1.3446 (3) Å is shorter in length than the aromatic carbon–carbon bonds [1.3911 (3)–1.4038 (3) Å], and might therefore be expected to be stronger, which is supported by the fact that the values of $\rho(r)$ [2.35 (1) e Å$^{-3}$] and $\nabla^2\rho(r)$ [−23.96 (3) e Å$^{-5}$] at the C7═C8 b.c.p. are larger in magnitude than for the C═C bonds within the aromatic ring.

[1] Supplementary data for this paper are available from the IUCr electronic archives (Reference: SO5021). Services for accessing these data are described at the back of the journal.

**Table 3**
Topological properties and geometrical parameters for the intermolecular hydrogen bond and weak C—H···O interactions in (1*a*).

Only one interaction is documented for those interactions with symmetry equivalents.

| *D*—H···*A* | $\rho(r)$ (e Å$^{-3}$) | $\nabla^2\rho(r)$ (e Å$^{-5}$) | H···*A* (Å) | *D*—A (Å) | *D*—H (Å) | *D*—H—*A* (°) |
|---|---|---|---|---|---|---|
| O1—H1*A*···O2$^{i}$ | 0.34 (1) | 4.85 (2) | 1.63 | 2.6328 (5) | 1.01 | 173 |
| C1—H1···O1$^{ii}$ | 0.03 (1) | 0.44 (1) | 2.87 | 3.4767 (4) | 1.08 | 116 |
| C2—H2···O1$^{ii}$ | 0.04 (1) | 0.76 (1) | 2.53 | 3.3296 (4) | 1.08 | 130 |
| C7—H7···O2$^{iii}$ | 0.03 (0) | 0.38 (0) | 2.92 | 3.5354 (4) | 1.08 | 116 |
| Ring | | | | | | |
| 2(1*a*)† | 0.05 | 0.9 | | | | |

Symmetry codes: (i) $-x, -y, 1-z$; (ii) $x, y, z-1$; (iii) $1+x, y, z$. † Ring 2(1*a*) = O2—C9—O1—H1*A*—O2$^{i}$—C9$^{i}$—O1$^{i}$—H1*A*$^{i}$.

**Table 4**
Topological properties at the b.c.p.s and r.c.p.s in (2*a*).

| Bond | *d* (Å) | $R_{ij}$ (Å)† | $\rho(r)$ (e Å$^{-3}$) | $\nabla^2\rho(r)$ (e Å$^{-5}$) | $\epsilon$ |
|---|---|---|---|---|---|
| C1—C2 | 1.3910 (2) | 1.3912 | 2.17 (1) | −18.77 (2) | 0.24 |
| C1—C6 | 1.3998 (2) | 1.3999 | 2.14 (1) | −18.21 (2) | 0.22 |
| C2—C3 | 1.3921 (2) | 1.3921 | 2.13 (1) | −17.22 (2) | 0.21 |
| C3—C4 | 1.4038 (2) | 1.4038 | 2.08 (1) | −16.37 (2) | 0.20 |
| C4—C5 | 1.3853 (2) | 1.3854 | 2.17 (1) | −18.81 (3) | 0.23 |
| C5—C6 | 1.4071 (2) | 1.4072 | 2.09 (1) | −16.71 (2) | 0.22 |
| C6—C7 | 1.4292 (2) | 1.4292 | 1.97 (1) | −15.16 (2) | 0.13 |
| C7—C8 | 1.3591 (2) | 1.3591 | 2.29 (1) | −20.85 (2) | 0.27 |
| C8—C9 | 1.4559 (2) | 1.4559 | 1.92 (1) | −14.95 (2) | 0.21 |
| C8—C10 | 1.4950 (2) | 1.4952 | 1.77 (1) | −11.97 (2) | 0.20 |
| C1—O1 | 1.3729 (2) | 1.3735 | 1.98 (1) | −14.57 (4) | 0.11 |
| C9—O1 | 1.3515 (2) | 1.3526 | 2.14 (1) | −19.91 (5) | 0.10 |
| C9—O2 | 1.2263 (2) | 1.2263 | 3.00 (1) | −39.37 (7) | 0.16 |
| C10—O3 | 1.3302 (2) | 1.3305 | 2.28 (1) | −21.40 (5) | 0.12 |
| C10—O4 | 1.2142 (2) | 1.2143 | 3.03 (1) | −35.85 (8) | 0.13 |
| C2—H2 | 1.08 | 1.08 | 1.84 (1) | −15.87 (4) | 0.04 |
| C3—H3 | 1.08 | 1.08 | 1.84 (1) | −16.53 (4) | 0.03 |
| C4—H4 | 1.08 | 1.08 | 1.89 (1) | −18.20 (4) | 0.05 |
| C5—H5 | 1.08 | 1.08 | 1.84 (1) | −16.68 (4) | 0.06 |
| C7–H7 | 1.08 | 1.08 | 1.85 (1) | −17.08 (4) | 0.04 |
| O3—H3*A* | 1.01 | 1.01 | 1.96 (2) | −23.6 (1) | 0.02 |
| Ring | | | | | |
| 1(2*a*)‡ | | | 0.16 | 3.2 | |
| 2(2*a*)§ | | | 0.16 | 3.2 | |

† $R_{ij}$ is the length of the bond path between atoms. ‡ Ring 1(2*a*) = C1—C2—C3—C4—C5—C6. § Ring 2(2*a*) = C1—C6—C7—C8—C9—O1.

Despite the fairly small C1—C6—C7—C8 torsion angle of 4.19 (5)°, significant delocalization between the two $\pi$ systems (aromatic and C7═C8) is not observed. The C6—C7 bond length of 1.4630 (3) Å is consistent with the average aromatic vinyl bond lengths in the Cambridge Structural Database (Allen, 2002) rather than being shortened, while C7═C8 is considerably shorter and stronger than the aromatic C—C bonds. This seems to agree with the findings of a theoretical charge-density investigation, which examined a series of cinnamic acids, including *trans*-cinnamic acid and concluded that the $\pi$ systems of the benzene ring and the propenoic acid fragment were independent with no delocalization in all of the cases studied (González Moa *et al.*, 2006).

At the time of reporting the structure of (1*a*) (Ladell *et al.*, 1956), it was noted that the molecules existed as hydrogen-bonded dimers, linked by carboxyl groups which straddle centres of symmetry. The anticipated strong intermolecular hydrogen bond O1—H1*A*···O2 was identified during this charge-density analysis along with three weak C—H···O interactions, Table 3. Examining the topological properties of the electron density at the b.c.p. corresponding to the H1*A*···O2 contact showed this to be a closed-shell interaction with a positive value of $\nabla^2\rho(r)$, and there is a clear charge concentration on the side of both O1 and O2 directed towards H1*A*, see Fig. 4. This type of relatively strong O—H···O hydrogen bonding is frequently observed with H1*A* remaining localized near to O1 (Hibbs *et al.*, 2003), however, in the extreme case the interaction becomes a linear ionic O···H···O hydrogen bond, with the H atom approximately equidistant between the two O atoms, as observed in the anions of 1,2,4,5-benzene-tetracarboxylic acid and 4,5-dichlorophthalic acid (Mallinson *et al.*, 2003).

### 3.2. Coumarin-3-carboxylic acid (2*a*)

The topological properties at the b.c.p.s for (2*a*) are provided in Table 4, and all expected covalent bonds were identified. The aromatic carbon bonds have similar topological properties [average $\rho(r)$ 2.13 (1) e Å$^{-3}$, average $\nabla^2\rho(r)$ −17.68 (3) e Å$^{-5}$] to those seen for (1*a*) and are consistent with those for aromatic bonds reported previously in the literature. The coumarin moiety (C1—C9/O1) is essentially planar with the atoms showing an r.m.s. deviation of 0.02 Å

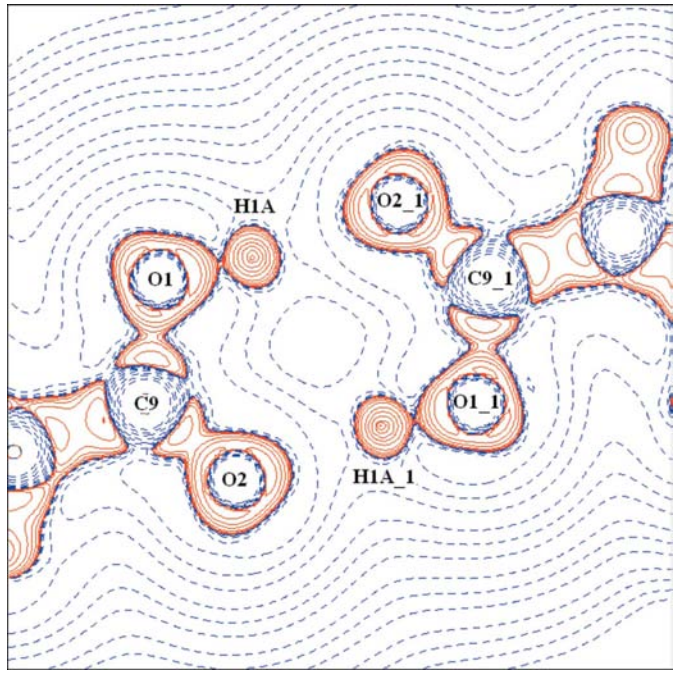


**Figure 4**
Laplacian of the electron density for (1*a*) drawn in the plane of the intermolecular O—H···O hydrogen bond. Positive contours are solid red lines, while negative contours are dashed blue lines; _1 = $-x, -y, 1-z$.

**Table 5**
Topological properties and geometrical parameters for the unique intramolecular hydrogen bond and weak C—H···O interactions in (2*a*).

| *D*—H···*A* | $\rho(r)$ (e Å$^{-3}$) | $\nabla^2\rho(r)$ (e Å$^{-5}$) | H···*A* (Å) | *D*—*A* (Å) | *D*—H (Å) | *D*—H—*A* (°) |
|---|---|---|---|---|---|---|
| O3—H3*A*···O2 | 0.29 (1) | 5.21 (1) | 1.64 | 2.5871 (3) | 1.01 | 154 |
| C5—H5···O4$^{i}$ | 0.04 (1) | 0.77 (1) | 2.48 | 3.4144 (2) | 1.08 | 144 |
| C7—H7···O4$^{i}$ | 0.05 (1) | 1.04 (1) | 2.35 | 3.3214 (2) | 1.08 | 149 |
| C3—H3···O3$^{ii}$ | 0.01 (0) | 0.15 (0) | 3.20 | 4.0168 (2) | 1.08 | 133 |
| C2—H2···O3$^{iii}$ | 0.02 (0) | 0.28 (0) | 2.92 | 3.8001 (3) | 1.08 | 139 |
| C3—H3···O4$^{iv}$ | 0.03 (0) | 0.46 (0) | 2.76 | 3.4983 (2) | 1.08 | 126 |
| C4—H4···O3$^{iv}$ | 0.03 (0) | 0.57 (0) | 2.63 | 3.4400 (2) | 1.08 | 131 |
| C5—H5···O1$^{v}$ | 0.03 (0) | 0.45 (0) | 2.97 | 3.3836 (2) | 1.08 | 103 |
| Ring 3(2*a*)† | 0.14 | 2.7 | | | | |

Symmetry codes: (i) $2-x,-1-y,1-z$; (ii) $\frac{1}{2}+x,\frac{1}{2}-y,z-\frac{1}{2}$; (iii) $\frac{3}{2}-x,\frac{1}{2}+y,\frac{1}{2}-z$; (iv) $\frac{1}{2}+x,-y-\frac{1}{2},z-\frac{1}{2}$; (v) $x,y-1,z$. † Ring 3(2*a*) C8—C10—O3—H3*A*—O2—C9.

from the least-squares plane containing these atoms. It is therefore not surprising to find evidence of delocalization between the two $\pi$ systems (aromatic ring and C7═C8), with the C6—C7 bond length of 1.4292 (2) Å being considerably shorter than the expected value of 1.47 Å. In addition, the values of $\rho(r)$ at 1.97 (1) e Å$^{-3}$ and $\nabla^2\rho(r)$ [−15.16 (2) e Å$^{-5}$] are higher than would be anticipated for a true single bond, whilst the values of of $\rho(r)$ 2.29 (1) e Å$^{-3}$ and $\nabla^2\rho(r)$ −20.85 (2) e Å$^{-5}$ for C7═C8 are lower than would be expected for a double bond [*cf. trans*-cinnamic acid $\rho(r)$ = 2.35 (1) e Å$^{-3}$, $\nabla^2\rho(r)$ = −23.96 (3) e Å$^{-5}$ for C7═C8]. It is also apparent that the C7═C8 bond length is slightly longer in (2*a*) than (1*a*), supporting increased delocalization [1.3591 (2) *versus* 1.3446 (3) Å]. A clear distinction can be seen between the single and double C—O bonds in terms of $\rho(r)$ and $\nabla^2\rho(r)$, with the values of both being considerably larger in magnitude for the C═O double bonds (C9═O2, C10═O4).

In the initial structural report for (2*a*) (Dobson & Gerkin, 1996) the presence of an intramolecular O—H···O hydrogen bond was noted, along with four short symmetry-related intermolecular C—H···O contacts. As expected, the O—H···O hydrogen bond is reasonably strong with a short *D*···*A* distance of 2.5871 (3) Å and a high density of 0.29 (1) e Å$^{-3}$ at the b.c.p., Table 5. The positive value in the Laplacian of 5.21 (1) e Å$^{-5}$ at the O—H···O b.c.p. classifies the interaction as closed-shell, and a small charge concentration can be seen in Fig. 5 on the side of both O1 and O2 directed towards H3*A*. In addition, seven bond paths corresponding to weak C—H···O interactions were identified.

### 3.3. Discussion

As mentioned in §1, whilst Schmidt's criteria derived from their pioneering studies in the 1960s can give an indication of compounds likely to undergo a solid state [2 + 2] cycloaddition reaction a number of exceptions to these rules have been identified. For example, while both 5-bromouracil (Sternglanz & Bugg, 1975) and maleic acid (Shahat, 1952) have parallel C═C double bonds separated by less than 4.2 Å, thus fulfilling Schmidt's criteria, neither showed signs of reacting after 3 d of irradiation. It has been postulated that their inertness may be explained by the presence of intermolecular hydrogen-bonding chains, which would be disrupted during such a reaction, along with/due to the small size of the molecules. Thus, any reaction would require significant movement of most of the atoms disrupting the crystal lattice (Mahon *et al.*, 2008).

Both *trans*-cinnamic acid [product (1*b*); Enkelmann *et al.*, 1993] and coumarin-3-carboxylic acid [product (2*b*); Mahon *et al.*, 2008] are known to undergo solid-state photo-induced [2 + 2] cycloaddition reactions. Examining the structures of (1*b*) and (2*b*) showed that on geometric grounds the strong hydrogen bonding appears to be maintained in the irradiation product. In the case of truxillic acid (1*b*) the intermolecular O···O separation is 2.639 Å with an O—H···O angle of 157°, whilst in (2*b*) the intramolecular O···O distance is 2.634 (5) Å and O—H···O angle is 135.3°. Of the weak C—H···O interactions, only one of the three unique contacts in (1*a*) [C1—H1···O1$^{i}$; (i) $x,y,z-1$] is likely to be sustained in the product, while in (2*b*) the C7—H7···O4$^{ii}$ [(ii) $2-x,-1-y,1-z$] and the C3—H3···O3$^{iii}$ [(iii) $\frac{1}{2}+x,\frac{1}{2}-y,z-\frac{1}{2}$] interactions are likely to be lost. Clearly charge-density studies would be required to confirm which interactions are lost or maintained. Although weak C—H···O interactions are likely to be lost in the formation of both (1*b*) and (2*b*), it is important to note that no strong intermolecular interactions have to be overcome for a reaction to occur.

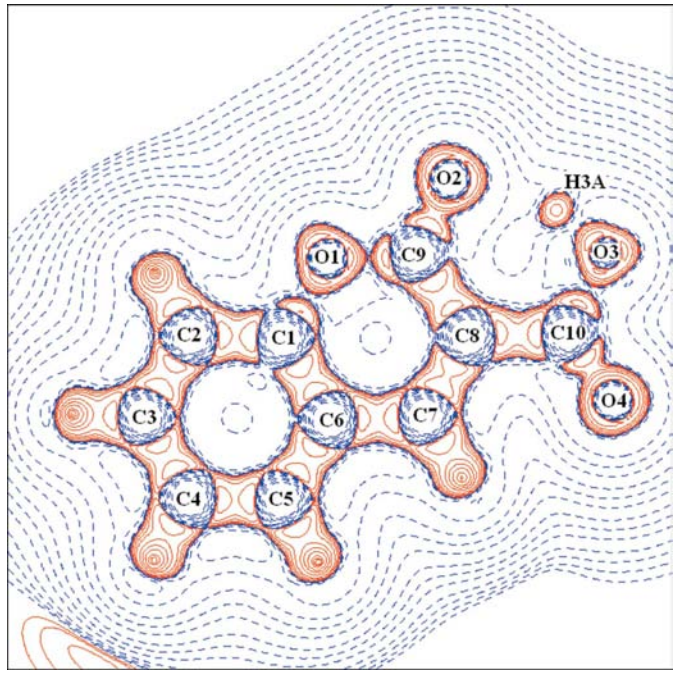


**Figure 5**
Laplacian of the electron density for (2*a*), positive contours are solid red lines, while negative contours are dashed blue lines.

**Table 6**
Topological properties for the unique weak intermolecular interactions between molecules in (1*a*) and (2*a*), only selected r.c.p.s provided.

| Bond | $\rho(r)$ (e Å$^{-3}$) | $\nabla^2\rho(r)$ (e Å$^{-5}$) | $d$ (Å) | $R_{ij}$ (Å)† |
|---|---|---|---|---|
| *trans*-Cinnamic acid | | | | |
| C1···C9$^{i}$ | 0.04 (1) | 0.44 (1) | 3.2728 (4) | 3.2883 |
| O1···C3$^{ii}$ | 0.02 (0) | 0.25 (0) | 3.5849 (5) | 3.5922 |
| O2···C2$^{ii}$ | 0.01 (0) | 0.20 (0) | 3.7999 (4) | 3.8070 |
| C6···H3$^{iii}$ | 0.04 (0) | 0.49 (0) | 2.8845 (2) | 2.9486 |
| C7···C4$^{iii}$ | 0.02 (0) | 0.29 (0) | 3.7560 (4) | 3.7590 |
| H2···H4$^{iv}$ | 0.02 (0) | 0.30 (0) | 2.6543 (4) | 2.7746 |
| C1···C4$^{v}$ | 0.04 (0) | 0.41 (0) | 3.5190 (4) | 3.5192 |
| C8···C5$^{v}$ | 0.04 (0) | 0.48 (0) | 3.4774 (3) | 3.4779 |
| O1···O1$^{vi}$ | 0.01 (0) | 0.24 (0) | 3.4656 (8) | 3.4656 |
| Ring | | | | |
| 3(1*a*)‡ | 0.03 | 0.4 | | |
| Coumarin-3-carboxylic acid | | | | |
| C7···C10$^{vii}$ | 0.04 (1) | 0.46 (1) | 3.2825 (2) | 3.4047 |
| O2···O1$^{viii}$ | 0.06 (1) | 0.99 (0) | 2.9269 (2) | 2.9383 |
| C2···H3$^{ix}$ | 0.03 (0) | 0.45 (0) | 2.9225 (2) | 3.0049 |
| C3···H5$^{x}$ | 0.04 (0) | 0.51 (0) | 2.8342 (2) | 2.8652 |
| O2···O4$^{xi}$ | 0.02 (0) | 0.39 (0) | 3.2725 (3) | 3.2859 |
| O2···C7$^{xi}$ | 0.04 (0) | 0.49 (0) | 3.2985 (2) | 3.3375 |
| C2···C5$^{xi}$ | 0.03 (0) | 0.41 (0) | 3.4819 (2) | 3.4847 |
| Ring | | | | |
| 4(2*a*)§ | 0.04 | 0.4 | | |

Symmetry codes: (i) $1-x,-y,2-z$; (ii) $x-1,y,z-1$; (iii) $x-\frac{1}{2},\frac{1}{2}-y,z-\frac{1}{2}$; (iv) $x-\frac{1}{2},\frac{1}{2}-y,\frac{1}{2}+z$; (v) $x-1,y,z$; (vi) $1-x,-y,1-z$; (vii) $x-1,y,z-1$; (viii) $\frac{3}{2}-x,\frac{1}{2}+y,\frac{1}{2}-z$; (ix) $2-x,-y,-z$; (x) $\frac{5}{2}-x,\frac{1}{2}+y,\frac{1}{2}-z$; (xi) $x,1+y,z$. † $R_{ij}$ is the length of the bond path between atoms. ‡ Ring 3(1*a*) = C1—C6—C7—C8—C9—C1$^{i}$—C6$^{i}$—C7$^{i}$—C8$^{i}$—C9$^{i}$. § Ring 4(2*a*) = C7—C8—C10—C7$^{xv}$—C8$^{xv}$—C10$^{xv}$; (xv) $2-x,-y,1-z$.

Clearly solid-state photo-induced [2 + 2] cycloaddition reactions occur in the excited state, however, intermolecular interactions in the ground state may have a significant influence on the ability of a molecule to react or not upon irradiation. In addition to the O—H···O hydrogen bonds and weak C—H···O interactions already documented (Tables 3 and 5), the charge-density analyses of (1*a*) and (2*a*) highlighted several other very weak intermolecular interactions all of comparable strength, see Table 6. In the case of (1*a*) only four of the interactions appear feasible in the irradiation product, while all of those identified in (2*a*) seem to be capable of being maintained upon irradiation.

In order to obtain further insight into the nature of the interactions, the Hirshfeld surfaces and fingerprint plots for the two structures were calculated using *CrystalExplorer* (Wolff *et al.*, 2007). The Hirshfeld surface partitions the space in a crystal into regions where the sum of the spherical-atom electron distribution for a specific molecule (the promolecule) dominates over the corresponding sum over the crystal (the procrystal). In this way distances from the surface to points inside ($d_i$) and outside ($d_e$) the surface can easily be calculated. However, these distances do not take into account the relative atomic sizes, hence short contacts between differently sized or large atoms are not effectively highlighted. To overcome this *CrystalExplorer* allows a normalized contact distance ($d_{norm}$), which incorporates the van der Waals radii of the appropriate atoms to be mapped onto the Hirshfeld surface to highlight

**Table 7**
Breakdown of the fingerprint plot given as percentages of the total Hirshfeld surface area.

| Contact | (1*a*) | (2*a*) |
|---|---|---|
| O···O | 0.3 | 5.1 |
| O···C | 2.4 | 16.8 |
| O···H | 26.3 | 32.5 |
| C···C | 4.0 | 2.7 |
| C···H | 27.8 | 21.6 |
| H···H | 39.1 | 21.3 |

contacts that are shorter (red), approximately equivalent to (white) or longer (blue) than the sum of the van der Waals radii. *CrystalExplorer* can also display fingerprint plots of $d_e$ *versus* $d_i$ for every point on the Hirshfeld surface; these provide a convenient two-dimensional representation of both the type of intermolecular contact present and the relative surface area accounted for by that type of interaction. White

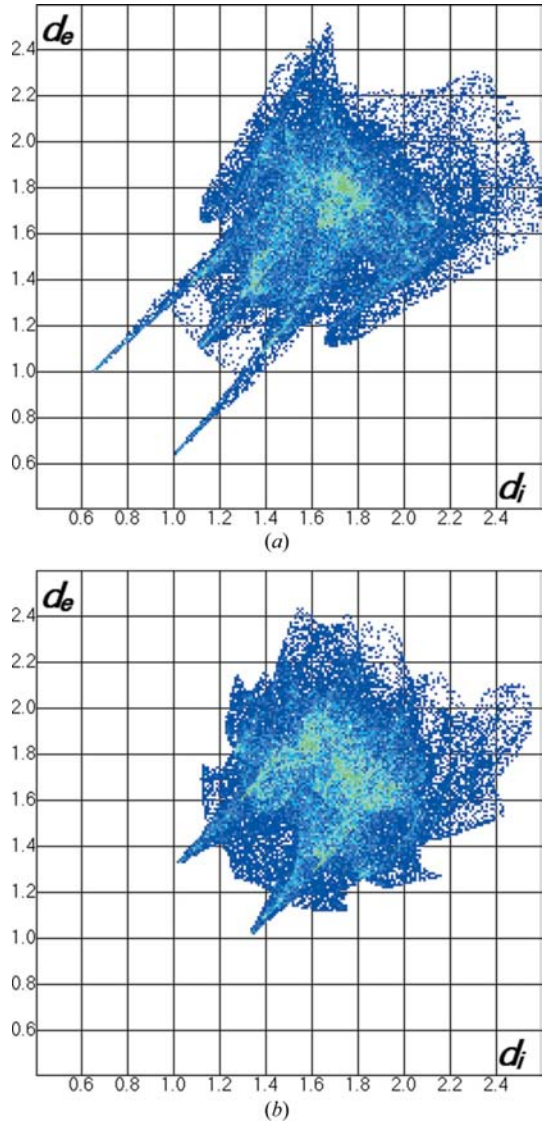


**Figure 6**
Fingerprint plot for (*a*) (1*a*) and (*b*) (2*a*).

areas indicate points with no contribution, blue through green to red represents the increasing contribution of a particular $d_e$–$d_i$ pair (McKinnon *et al.*, 2007). Table 7 provides a breakdown of the fingerprint plots given in Fig. 6. The off-diagonal spikes extending down to $\sim 0.6$ in either $d_e$ and $d_i$ are indicative of strong O—H···O hydrogen bonding in (1*a*). In addition, the spikes along the diagonal in (1*a*) are due to the presence of short H···H contacts, whilst the wings arise from C—H···$\pi$ interactions. Interestingly, examining the Hirshfeld surfaces for contacts shorter than the van der Waals radii of the atoms (depicted in red) highlights short C···C contacts in addition to the hydrogen-bonding interactions, see Fig. 7. These C···C contacts are between pairs of molecules that react upon irradiation, C1—C9$^{i}$ in (1*a*) and C7—C10$^{ii}$ in (2*a*) [(i) $1-x, -y, 2-z$; (ii) $x-1, y, z-1$], and were identified in Table 6 (Fig. 8). These weak interactions are not located directly between the two potentially reactive C7═C8 bonds, and may not be related to a compound's ability to undergo a [2 + 2] cycloaddition. However, it is worth noting that the electrostatic potentials (calculated in *CrystalExplorer*; Wolff *et al.*, 2007) around the atoms involved have opposite signs in both cases. This means that electropositive regions [C1/C1$^{i}$ in (1*a*) and C7/C7$^{ii}$ in (2*a*)] lie adjacent to complementary electronegative regions [C9/C9$^{i}$ in (1*a*) and C10/C10$^{ii}$ in (2*a*)] and may provide some explanation for the tendency of these pairs of molecules to dimerize upon irradiation. Further charge-density studies are currently being undertaken to determine whether such interactions exist in other compounds which undergo [2 + 2] cycloaddition reactions upon irradiation and whether they are absent in compounds which do not react but appear suited to reaction upon geometrical grounds.

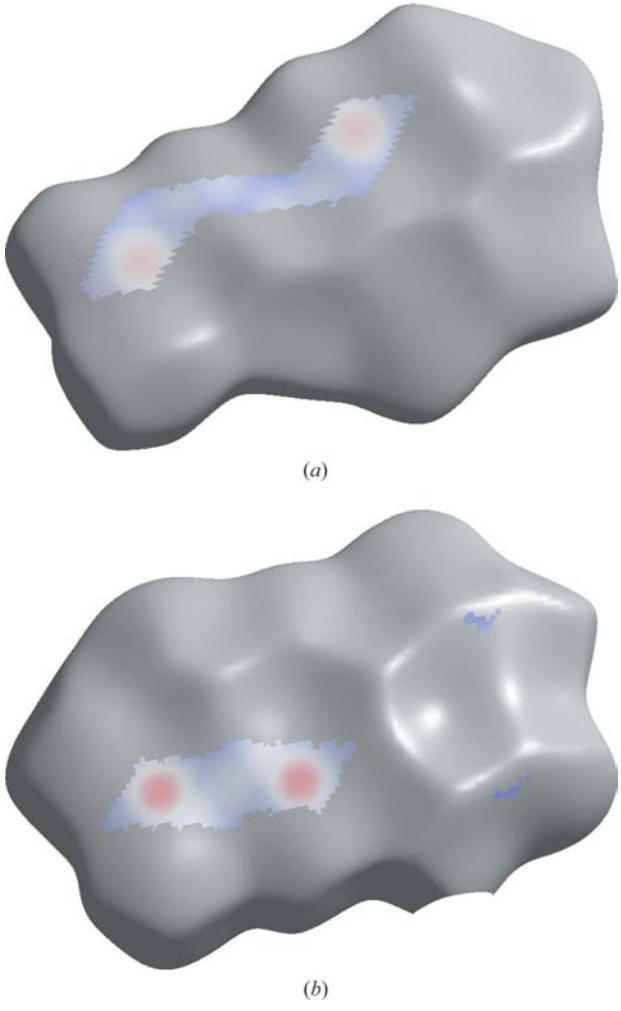


**Figure 7**
Hirshfeld surface $d_{norm}$ with short C···C contacts depicted in red for (*a*) (1*a*) and (*b*) (2*a*). Full plot can be found as Fig. S5 in the supplementary material.

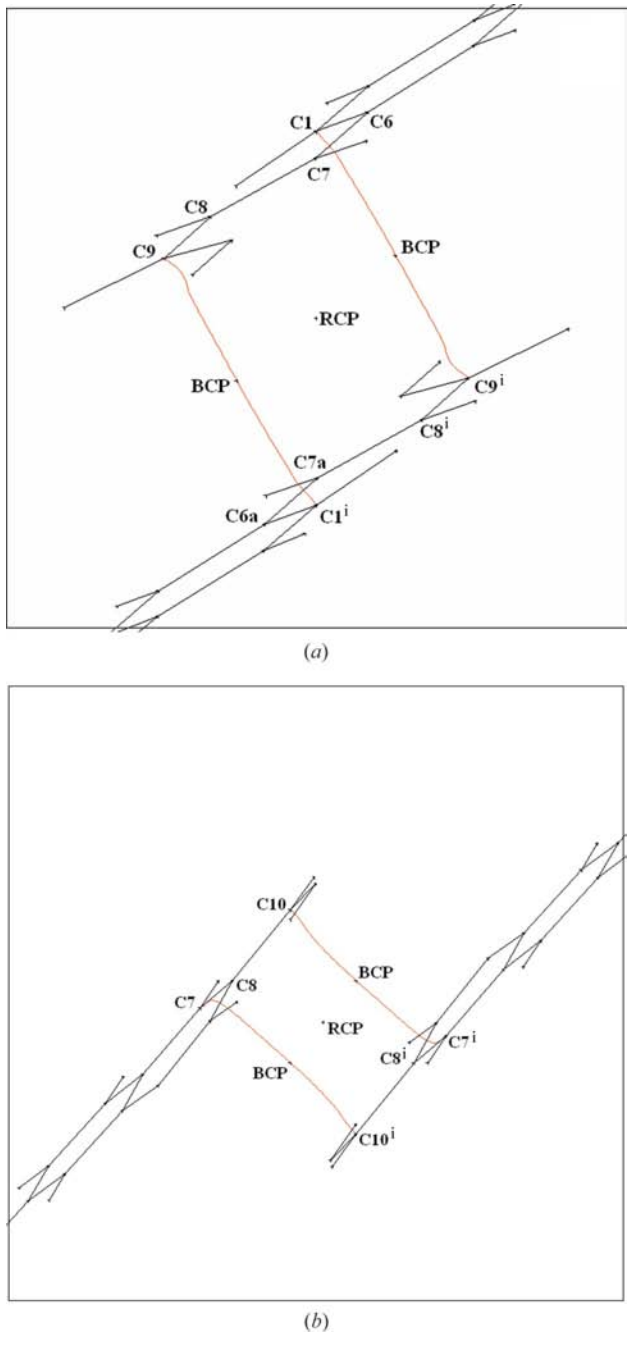


**Figure 8**
Illustration of the bond paths for the interactions between potentially reactive molecules, symmetry equivalent atoms (*a*) in (1*a*) (i) $1-x, -y, 2-z$, (*b*) in (2*a*) (i) $2-x, -y, 1-z$.

## 4. Conclusions

The experimental low-temperature charge-density analyses of *trans*-cinnamic acid and coumarin-3-carboxylic acid afforded a good refinement. All expected intramolecular b.c.p.s and r.c.p.s were identified and analysed using AIM methods, and found to fit an open-shell, *i.e.* covalent description. The anticipated strong hydrogen bonds were identified in both (1*a*) and (2*a*) and classified as localized closed-shell interactions. The topological properties of the hydrogen bond were comparable to values found for similar interactions in the literature (Scheins *et al.*, 2005). Some delocalization of the two $\pi$ systems (aromatic and C═C) was observed in coumarin-3-carboxylic acid, but was less apparent in *trans*-cinnamic acid.

We postulate that the presence of strong intra- or intermolecular interactions, which cannot be maintained in the irradiation product, may influence the ability of a compound to undergo a solid-state [2 + 2] cycloaddition reaction. In the case of both (1*a*) and (2*a*), it is worth noting that the strong hydrogen-bonding interactions and the majority of the weak interactions can be maintained in their irradiation products, and importantly no strong interactions are lost. The significance of the C$\cdots$C contacts, shorter than the sum of the van der Waals radii, between pairs of potentially reactive ground-state molecules combined with their differing electrostatic potentials is currently undergoing further investigation.

The authors are very grateful to Dr Zoltán Gál of Oxford Diffraction Ltd for collecting the charge-density data and would like to thank the EPSRC for funding (EP/E048994/1). PRR is also grateful to the EPSRC for the award of a Senior Fellowship.

## References

Allen, F. H. (2002). *Acta Cryst.* B**58**, 380–388.
Bader, R. F. W. (1990). *Atoms in Molecules, A Quantum Theory*. Oxford University Press.
Bader, R. F. W., Tang, T.-H., Tal, Y. & Biegler-König, F. W. (1982). *J. Am. Chem. Soc.* **104**, 946–952.
Blessing, R. H. (1997). *J. Appl. Cryst.* **30**, 421–426.
Dobson, A. J. & Gerkin, R. E. (1996). *Acta Cryst.* C**52**, 3081–3083.
Enkelmann, V., Wegner, G., Novak, K. & Wagener, K. B. (1993). *J. Am. Chem. Soc.* **115**, 10390–10391.
Farrugia, L. J. (1999). *J. Appl. Cryst.* **32**, 837–838.
González Moa, M. J., Mandado, M. & Mosquera, R. A. (2006). *Chem. Phys. Lett.* **424**, 17–22.
Hansen, N. K. & Coppens, P. (1978). *Acta Cryst.* A**34**, 909–921.
Hibbs, D. E., Overgaard, J. & Piltz, R. O. (2003). *Org. Biomol. Chem.* **1**, 1191–1198.
Hirshfeld, F. L. (1976). *Acta Cryst.* A**32**, 239–244.
Ladell, J., McDonald, T. R. R. & Schmidt, G. M. J. (1956). *Acta Cryst.* **9**, 195.
Madsen, A. Ø. (2006). *J. Appl. Cryst.* **39**, 757–758.
Mahon, M. F., Raithby, P. R. & Sparkes, H. A. (2008). *CrystEngComm*, **10**, 573–576.
Mallinson, P. R., Smith, G. T., Wilson, C. C., Grech, E. & Wozniak, K. (2003). *J. Am. Chem. Soc.* **125**, 4259–4270.
McKinnon, J. J., Jayatilaka, D. & Spackman, M. A. (2007). *Chem. Commun.* pp. 3814–3816.
Ramamurthy, V. & Venkatesan, K. (1987). *Chem. Rev.* **87**, 433–481.
Scheins, S., Messerschmidt, M. & Luger, P. (2005). *Acta Cryst.* B**61**, 443–448.
Schmidt, G. M. J. & Cohen, M. D. (1964). *J. Chem. Soc.* pp. 1996–2000.
Shahat, M. (1952). *Acta Cryst.* **5**, 763–768.
Sheldrick, G. M. (2008). *Acta Cryst.* A**64**, 112–122.
Sternglanz, H. & Bugg, C. E. (1975). *Biochim. Biophys. Acta*, **378**, 1–11.
Volkov, A., Macchi, P., Farrugia, L. J., Gatti, C., Mallinson, P., Richter, T. & Koritsanszky, T. (2006). *XD*2006. University at Buffalo, State University of New York, NY, USA; University of Milano, Italy; University of Glasgow, UK; CNRISTM, Milano, Italy; Middle Tennessee State University, TN, USA.
Wolff, S. K., Grimwood, D. J., McKinnon, J. J., Jayatilaka, D. & Spackman, M. A. (2007). *CrystalExplorer*2.1. University of Western Australia, http://hirshfeldsurface.net/CrystalExplorer.